

**Electronic Supplementary Information for**  
**Photodelivery of  $\beta$ -phenylethylamines**

*Sumin Lee, Seung Yeon Yi and Youngmin You\**

Division of Chemical Engineering and Materials Science, Ewha Womans University, Seoul 03760,  
Republic of Korea.

\*To whom correspondence should be addressed: [odds2@ewha.ac.kr](mailto:odds2@ewha.ac.kr)

---

|                      |   |
|----------------------|---|
| Experimental details | S1  |
| References           | S6  |
| <b>Fig. S1</b>       | Photophysical behaviors of the DPSY compounds S7                                      |
| <b>Fig. S2</b>       | Photoluminescence decay traces S8   |
| <b>Fig. S3</b>       | Comparison of the $^1\text{H}$ NMR spectra S9   |
| <b>Fig. S4</b>       | $^1\text{H}$ NMR spectra (300 MHz) of DPSY2 S10                                       |
| <b>Fig. S5</b>       | Liquid chromatograms S11  |
| <b>Fig. S6</b>       | Control experiments of photouncaging PEA S12  |
| <b>Fig. S7</b>       | Variable-wavelength photouncaging of PEA S13  |
| <b>Fig. S8</b>       | Comparisons of the UV-vis absorption spectra S14                                      |
| <b>Fig. S9</b>       | Comparisons of the changes in the UV-vis absorption spectra S15                       |
| <b>Fig. S10</b>      | Distributions of the diameter of the DMPC liposomes S16                               |
| <b>Fig. S11</b>      | Surface charge of the DMPC liposomes S17  |
| <b>Fig. S13</b>      | Determination of an efficiency for the encapsulation of DPSY1 S18                     |
| <b>Fig. S13</b>      | Calibration curve of the ninhydrin test for $\beta$ -phenylethylamine S19             |
| <b>Fig. S14</b>      | $^1\text{H}$ NMR (300 MHz, $\text{CD}_2\text{Cl}_2$ ) spectrum of DPSY1 S20           |
| <b>Fig. S15</b>      | $^{13}\text{C}\{^1\text{H}\}$ NMR (126 MHz, $\text{DMSO}-d_6$ ) spectrum of DPSY1 S21 |
| <b>Fig. S16</b>      | $^1\text{H}$ NMR (300 MHz, $\text{DMSO}-d_6$ ) spectrum of DPSY2 S22                  |
| <b>Fig. S17</b>      | $^{13}\text{C}\{^1\text{H}\}$ NMR (126 MHz, $\text{DMSO}-d_6$ ) spectrum of DPSY2 S23 |

**Experimental Details**

**Materials and General Methods.** Commercially available chemicals were used as received unless otherwise stated. 2-Benzoylbenzophenone (97.0%) was purchased from Alfa Aesar.  $\beta$ -Phenylethylamine (>98.0%), (*R*)-(+)- $\beta$ -methylphenylethylamine (>98.0%), and 1,2-dimyristoyl-*sn*-glycero-3-phosphocholine (DMPC, >97.0%) were purchased from Tokyo Chemical Industry. Sodium borohyride (99.0%), ninhydrin, and anhydrous methanol (99.8%) were purchased from

Sigma–Aldrich. Irppy was prepared following the literature procedure.<sup>1</sup> <sup>1</sup>H and <sup>13</sup>C{<sup>1</sup>H} NMR spectra were collected with Bruker, Ultrashield 500, 400 and 300 plus NMR spectrometers. Chemical shifts were referenced to (CH<sub>3</sub>)<sub>4</sub>Si. High resolution mass spectra (positive mode, EI) were obtained by employing a JEOL, JMS-600W mass spectrometer.

**Synthesis of DPSY1.** DPSY1 was synthesized in two-step synthesis.<sup>2</sup> 2-Benzoylbenzophenone (0.50 g, 1.75 mmol) and β-phenylethylamine (0.47 g, 3.85 mmol) were added into a 100 mL, 2-necked round-bottom flask equipped with a magnetic stir bar. Anhydrous methanol (50 mL) was delivered into the flask using a glass syringe under an Ar atmosphere, and then, the reaction mixture was heated at 80°C for 24 h. After cooling to room temperature, NaBH<sub>4</sub> (0.13 g, 3.5 mmol) was added and the reaction mixture was stirred at room temperature for additional 5 h. The reaction was quenched by pouring the solution onto ice water. The reaction mixture was diluted by adding 100 mL water, and the crude product was extracted with EtOAc. The organic layer was dried over anhydrous MgSO<sub>4</sub> and concentrated under a reduced pressure. Column purification was performed on silica gel using hexane:EtOAc = 19:1 (v/v) as an eluent to afford DPSY1 as a yellow powder in a 23% yield. *R*<sub>f</sub> = 0.7 (hexane:EtOAc = 3:1, v/v). <sup>1</sup>H NMR (300 MHz, CD<sub>2</sub>Cl<sub>2</sub>) δ (ppm): 2.56 (t, *J* = 7.7 Hz, 2H), 4.60 (t, *J* = 7.5 Hz, 2H), 6.54–6.57 (m, 2H), 6.87–6.91 (m, 2H), 7.07–7.09 (m, 3H), 7.36–7.59 (m, 12H). <sup>13</sup>C{<sup>1</sup>H} NMR (126 MHz, DMSO-*d*<sub>6</sub>) δ (ppm): 16.77, 47.71, 119.60, 122.38, 123.11, 124.09, 127.10, 127.88, 128.78, 128.97, 129.57, 130.56, 132.64, 138.23. HR MS (EI<sup>+</sup>): Calcd for C<sub>28</sub>H<sub>23</sub>N ([M+H]<sup>+</sup>), 373.1830; found, 373.1833.

**Synthesis of DPSY2.** DPSY2 was prepared, following the method identical to DPSY1. Column purification on silica gel using hexane:EtOAc = 7:1 (v/v) as an eluent afforded DPSY2 as a yellow powder in a 20% yield. *R*<sub>f</sub> = 0.4 (hexane:EtOAc = 3:1, v/v). <sup>1</sup>H NMR (300 MHz, DMSO-*d*<sub>6</sub>) δ (ppm): 0.64 (d, *J* = 7.2 Hz, 3H), 4.46-4.64 (m, 3H), 6.49 (dd, *J* = 7.5, 1.8 Hz, 2H), 6.88 (dd, *J* = 6.6, 3.0 Hz, 2H), 7.02-7.08 (m, 3H), 7.40 (dd, *J* = 6.6, 3.0 Hz, 2H), 7.38-7.46 (m, 2H), 7.51-7.60 (m, 8H). <sup>13</sup>C{<sup>1</sup>H} NMR (126 MHz, DMSO-*d*<sub>6</sub>) δ (ppm): 17.21, 53.01, 118.94, 121.76, 122.29, 124.05, 126.28, 126.46, 126.99, 128.20, 128.90, 129.71, 132.10, 142.45. HR MS (EI<sup>+</sup>): Calcd for C<sub>28</sub>H<sub>23</sub>N ([M+H]<sup>+</sup>), 387.1987; found, 387.1992.

**Preparation of Liposomes.** Fresh liposomes doped with DPSY1 and Irppy were prepared prior to each measurement. 33.9 mg of DMPC, 7.5 mg of DPSY1, and 1.65 mg of Irppy were fully dissolved in a 5 mL chloroform:methanol (1:4, v/v) solution in a 20 mL glass vial.<sup>3</sup> Concentrations of DPSY1

and Irppy corresponded to 4 mM and 0.8 mM, respectively. Slow removal of the solvent with employing a rotavap yielded a thin lipid film coated inside the vial. Then, 5 mL of Milli-Q water was added into the vial. The mixture was vigorously vortexed and, then, sonicated for 5 min. The hazy suspension was filtered using a cellulose acetate filter (pore size = 0.45  $\mu\text{m}$ ). Centrifugation was performed at 2000 rpm at 20°C for 30 min using a UNION 32R PLUS instrument (Hanil, Korea). The supernatant was carefully decanted. Milli-Q water was subsequently added, and the centrifugation–decantation cycle was repeated.

**Determination of Encapsulation Efficiency of DPSY1 Within Liposomes.** 1 mL of a as-prepared liposome suspension was taken before centrifugation. The solution was delivered into a 15 mL conical tube, and centrifuged at 2000 rpm at 20°C for 30 min. Supernatant and liposome aggregates were separated, and their UV–vis absorption spectra were collected. The efficiency of encapsulation was calculated based on the 372 nm absorbance of DPSY1, through the relationship, efficiency of encapsulation (%) =  $100 \times (\text{absorbance}(372 \text{ nm}) \text{ of liposome aggregates}) / (\text{absorbance}(372 \text{ nm}) \text{ of liposome aggregates} + \text{absorbance}(372 \text{ nm}) \text{ of supernatant})$ .

**Steady-State UV–vis Absorption Measurements.** UV–vis absorption spectra were collected on an Agilent, Cary 300 spectrophotometer at 298 K. Sample solutions were prepared prior to measurements at a concentration of 10  $\mu\text{M}$  in toluene, unless otherwise stated. The solution was delivered into a quartz cell (Hellma, beam path length = 1.0 cm).

**Steady-State Photoluminescence Measurements.** Photoluminescence spectra were obtained using a Photon Technology International, Quanta Master 400 scanning spectrofluorometer at 298 K. The solutions used for the steady-state UV–vis absorption studies were employed for the photoluminescence measurements. A quartz cell (Hellma, beam path length = 1.0 cm) was employed. The photoluminescence spectra were recorded in the emission range 350–700 nm.

**ATR FT–IR Measurement.** ATR FT–IR measurements were performed for a powdery sample of DPSY1 and Irppy (100:1, mol/mol) with an Agilent, Cary 630 FT–IR spectrometer. The sample was prepared by dissolving 1 mM DPSY1 and 10  $\mu\text{M}$  Irppy in  $\text{CH}_3\text{CN}$ . The solution was photoirradiated at a wavelength of 365 nm with a UV lamp (4 W), after which the solvent was removed employing a rotavap.

**Determination of Photoluminescence Lifetimes.** Deaerated toluene solutions of 10  $\mu\text{M}$  sample were employed. Photoluminescence decay traces were acquired based on time-correlated single-photon-counting (TCSPC) techniques, using a PicoQuant, FluoTime 200 instrument after picosecond pulsed laser excitation at 377 nm. Transient photon signals were collected at  $\lambda_{\text{obs}} = 455$  nm (DPSY1) or 458 nm (DPSY2) through an automated motorized monochromator. The photon acquisition was terminated when the accumulated photon count reached  $10^4$ . Photoluminescence decay traces were analyzed using a monoexponential decay model embedded in an OriginLab, OriginPro 2018 software.

**Determination of Relative Photoluminescence Quantum Yields.** The relative photoluminescence quantum yield (PLQY) was determined for the solutions, following the equation  $\text{PLQY} = \text{PLQY}_{\text{ref}} \times (I/I_{\text{ref}}) \times (A_{\text{ref}}/A) \times (n/n_{\text{ref}})^2$ , where  $A$ ,  $I$ , and  $n$  are the absorbance at the excitation wavelength, the integrated photoluminescence intensity, and the refractive index of the solvent, respectively. 9,10-Diphenylanthracene ( $\text{PLQY}_{\text{ref}} = 1.00$ ;  $\lambda_{\text{ex}} = 366$  nm) was used as the reference material.<sup>4</sup> 10  $\mu\text{M}$  samples or the reference were dissolved in toluene (spectrophotometric grade). Photoluminescence spectra were collected at 298 K in the emission range 350–700 nm. The spectra were integrated with employing an OriginLab, OriginPro 2018 software.

**HPLC Experiments.** An  $\text{O}_2$ -saturated  $\text{CH}_3\text{CN}$  solution (3 mL) containing 1.0 mM DPSY1 and 100  $\mu\text{M}$  Irppy was photoirradiated at 365 nm with a UV lamp (4 W). An aliquot of 300  $\mu\text{L}$  was taken from the solution during the course of continuous photoirradiation, and was injected into an Agilent, 6120DW LC/MSD instrument equipped with a Poroshell, EC-C18 column ( $2.1 \times 100$  mm, 2.7  $\mu\text{m}$ ) through an autosampler. Eluent was gradiently changed from  $\text{H}_2\text{O}:\text{CH}_3\text{CN} = 40:60$  (v/v) to  $\text{CH}_3\text{CN}$ . A UV (254 nm) detector was employed. Chromatographic peaks corresponding to DPSY1, Irppy, the  $^1\text{O}_2$ -oxidation product of DPSY1, and  $\beta$ -phenylethylamine were observed at elution times of 19.83, 8.68, 7.08, and 0.67 min, respectively. Mass analyses were subsequently carried out through an electrospray nebulizer. Positive ions were detected in the  $m/z$  range 150–2000.

**Dynamic Light Scattering Experiments.** Distributions of the diameter of DMPC liposomes were determined through dynamic light scattering (DLS) experiments by using a Photall Otsuka Electronics, DLS-7000 instrument at room temperature. Data analyses were performed with employing the software provided by the manufacturer.

**Electrophoretic Light Scattering Experiments.** Zeta potentials of the DMPC liposomes were determined through electrophoretic light scattering experiments by using an Otsuka Portal, ELS-Z1000 instrument at room temperature. Data analyses were performed with employing the software provided by the manufacturer.

**Ninhydrin Test.** A 10 mM ninhydrin and a 100 mM  $\beta$ -phenylethylamine were dissolved in DMF. 2 mL of the ninhydrin solution was mixed with different amounts of the  $\beta$ -phenylethylamine solution (0, 0.5, 1.0, 1.5, 2.0, and 2.5 mM), and the mixtures were heated at 80°C for 5 min using a waterbath.<sup>5</sup> After cooling to room temperature, the treated solutions were diluted in DMF to one tenth. The solution was inserted into a 1 mm-thick quartz cell for UV-vis absorption measurements. An emergence of an absorption band at  $\lambda_{\text{abs}} = 613$  nm corresponded to Ruhemann's purple, the product of the reaction between  $\beta$ -phenylethylamine and ninhydrin. In order to quantify the photoreleased  $\beta$ -phenylethylamine, a calibration curve was constructed.

**Determination of photochemical quantum yields.** The quantum yields for the photoinduced release of amines from the DPSY compounds were determined by the standard ferrioxalate actinometry. A 0.0060 M  $\text{K}_3[\text{Fe}(\text{C}_2\text{O}_4)_3]$  solution served as the chemical actinometer. 500  $\mu\text{L}$  of the  $\text{K}_3[\text{Fe}(\text{C}_2\text{O}_4)_3]$  solution was transferred to a 1 cm  $\times$  1 mm quartz cell, and the solution was photoirradiated at a wavelength of 365 nm with a hand-held UV lamp (4 W) for 20 s. Then same amount of 1 % 1,10-phenanthroline in sodium acetate buffer (4.09 g  $\text{CH}_3\text{COONa}$  dissolved in 18 mL of 0.5 M  $\text{H}_2\text{SO}_4$  and 32 mL of milli-Q water) were added and stored under dark for 1 h. The absorbance change at 510 nm was recorded. Inserting the value to eq. 1 returned the light intensity value of  $2.3 \times 10^{-8}$  einstein  $\text{s}^{-1}$ :

$$\text{Light intensity } (I_0, \text{ einstein s}^{-1}) = (\Delta\text{Abs}(510 \text{ nm}) \times V) / (\text{QY} \times 11050 \text{ M}^{-1} \text{ cm}^{-1} \times \Delta t) \quad (\text{eq. 1}).$$

In eq. 1,  $\Delta\text{Abs}(510 \text{ nm})$ ,  $V$ ,  $\text{QY}$ , and  $\Delta t$  are the absorbance change at 510 nm, volume (L), the quantum yield (1.1) of the ferrioxalate actinometer at 420 nm,<sup>6</sup> and photoirradiation time (s), respectively. The photogenerated  $\beta$ -phenylethylamine ([PEA]) was quantified through the calibration curve of the ninhydrin test, and was inserted into eq. 2:

$$\text{QY} = ([\text{PEA}] \times V) / (I_0 \times \Delta t) \quad (\text{eq. 2})$$

In eq. 2,  $\Delta t$  (s) is the photoirradiated time,  $V$  is the volume of the solution (L), and  $I_0$  are the light intensity obtained by eq. 1 (einstein  $s^{-1}$ ).

**Quantum chemical calculations.** Geometry optimization was performed using the Coulomb-attenuated method Becke's three-parameter CAM-B3LYP exchange-correlation functional and the 6-311+G(d,p) basis set. Frequency calculations were subsequently performed to assess the stability of the convergence. Time-dependent density functional theory (TD-DFT) calculations were carried out for the optimized geometries using the same functional and basis sets. Geometry optimization and single-point calculations were performed using the Gaussian 09 program.<sup>7</sup>

## References

1. H. Woo, S. Cho, Y. Han, W. S. Chae, D.-R. Ahn, Y. You, and W. Nam, *J. Am. Chem. Soc.*, 2013, **135**, 4771–4787.
2. D. T. Hsu, and C. H. Lin, *J. Org. Chem.*, 2009, **74**, 9180–9187.
3. Liposome Preparation - Avanti® Polar Lipids, <https://www.sigmaaldrich.com/technical-documents/articles/biology/liposome-preparation.html>, (accessed June, 2018).
4. G. Heinrich, S. Schoof and H. Gusten, *J. Photochem.*, 1974, **3**, 315–320.
5. V. P. Patil, S. J. Devdhe, R. V. Kawde, V. S. Kulkarni, V. J. Nagmoti, R. D. Patil, and S. H. Kale, *Int. J. Pharm. Pharm. Sci.*, 2012, **4**, 711–713.
6. H. J. Kuhn, S. E. Braslavsky, and R. Schmidt, *Pure Appl. Chem.*, 2004, **76**, 2105-2146.
7. M. J. Frisch, G. W. Trucks, H. B. Schlegel, G. E. Scuseria, M. A. Robb, J. R. Cheeseman, G. Scalmani, V. Barone, B. Mennucci, G. A. Petersson, H. Nakatsuji, M. Caricato, X. Li, H. P. Hratchian, A. F. Izmaylov, J. Bloino, G. Zheng, J. L. Sonnenberg, M. Hada, M. Ehara, K. Toyota, R. Fukuda, J. Hasegawa, M. Ishida, T. Nakajima, Y. Honda, O. Kitao, H. Nakai, T. Vreven, J. J. A. Montgomery, J. E. Peralta, F. Ogliaro, M. Bearpark, J. J. Heyd, E. Brothers, K. N. Kudin, V. N. Staroverov, T. Keith, R. Kobayashi, J. Normand, K. Raghavachari, A. Rendell, J. C. Burant, S. S. Iyengar, J. Tomasi, M. Cossi, N. Rega, J. M. Millam, M. Klene, J. E. Knox, J. B. Cross, V. Bakken, C. Adamo, J. Jaramillo, R. Gomperts, R. E. Stratmann, O. Yazyev, A. J. Austin, R. Cammi, C. Pomelli, J. W. Ochterski, R. L. Martin, K. Morokuma, V. G. Zakrzewski, G. A. Voth, P. Salvador, J. J. Dannenberg, S. Dapprich, A. D. Daniels, O. Farkas, J. B. Foresman, J. V. Ortiz, J. Cioslowski, and D. J. Fox, Gaussian 09, Gaussian, Inc.: Wallingford, CT, 2009.

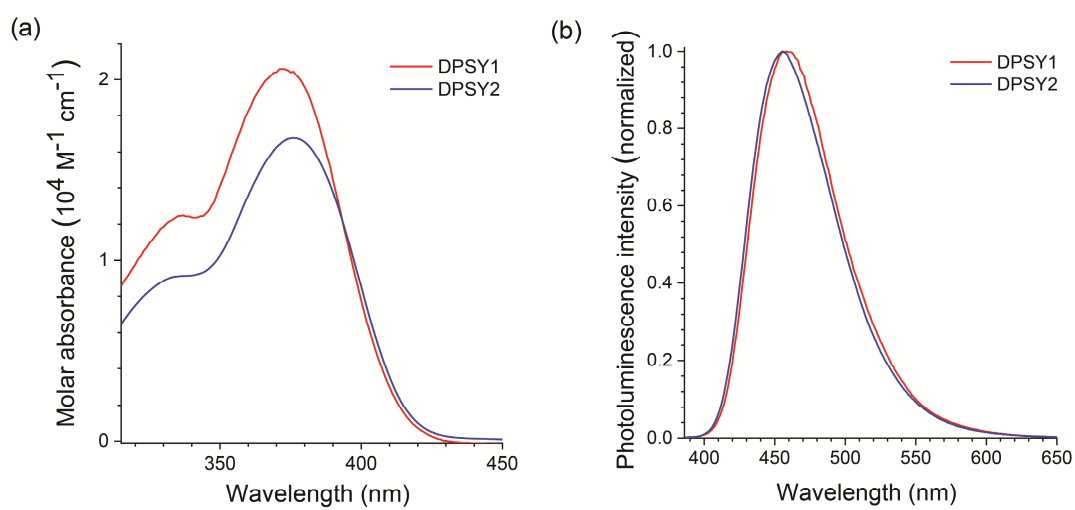


**Fig. S1** Photophysical behaviors of the DPSY compounds. (a) UV-vis absorption and (b) photoluminescence (normalized to 1) spectra of 10  $\mu\text{M}$  DPSY1 (red) and 10  $\mu\text{M}$  DPSY2 (blue) obtained in toluene. Excitation wavelengths = 373 nm (DPSY1) and 375 nm (DPSY2).

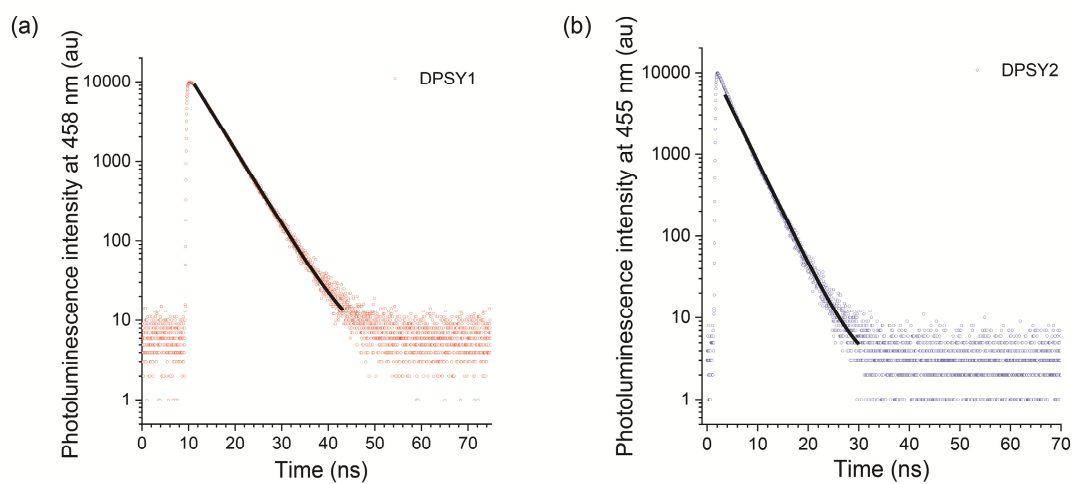


**Fig. S2** Photoluminescence decay traces of 10  $\mu\text{M}$  DPSY1 (a,  $\lambda_{\text{obs}} = 458 \text{ nm}$ ) and 10  $\mu\text{M}$  DPSY2 (b,  $\lambda_{\text{obs}} = 455 \text{ nm}$ ) in Ar-saturated toluene after picosecond pulsed laser excitation at 377 nm. The black solid lines correspond to the non-linear least-squares fits of the decay traces to a monoexponential decay model. Fluorescence lifetime ( $\tau_{\text{obs}}$ ) values are listed in the main text, Table 1.

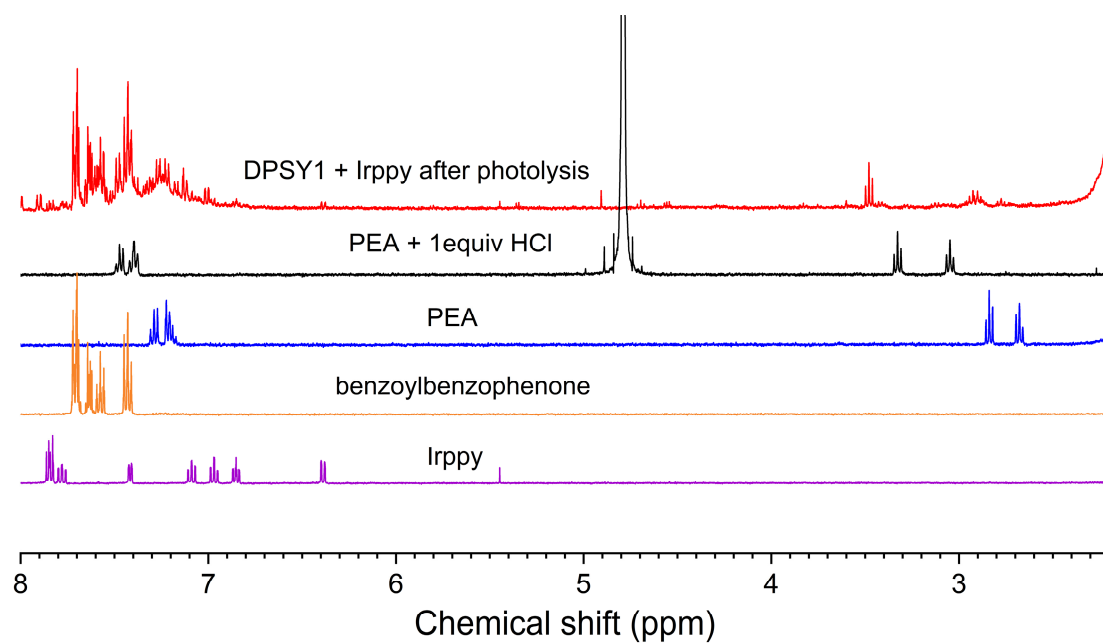


**Fig. S3** Comparison of the <sup>1</sup>H NMR spectrum (400 MHz) of photoirradiated (365 nm) CD<sub>3</sub>CN containing 3.0 mM DPSY1 and 100 μM Irppy (red) with the spectra (400 MHz, CD<sub>3</sub>CN) of 2-benzoylbenzophenone (orange), Irppy (violet), and PEA in the presence (black) and absence (blue) of 1 equiv HCl.

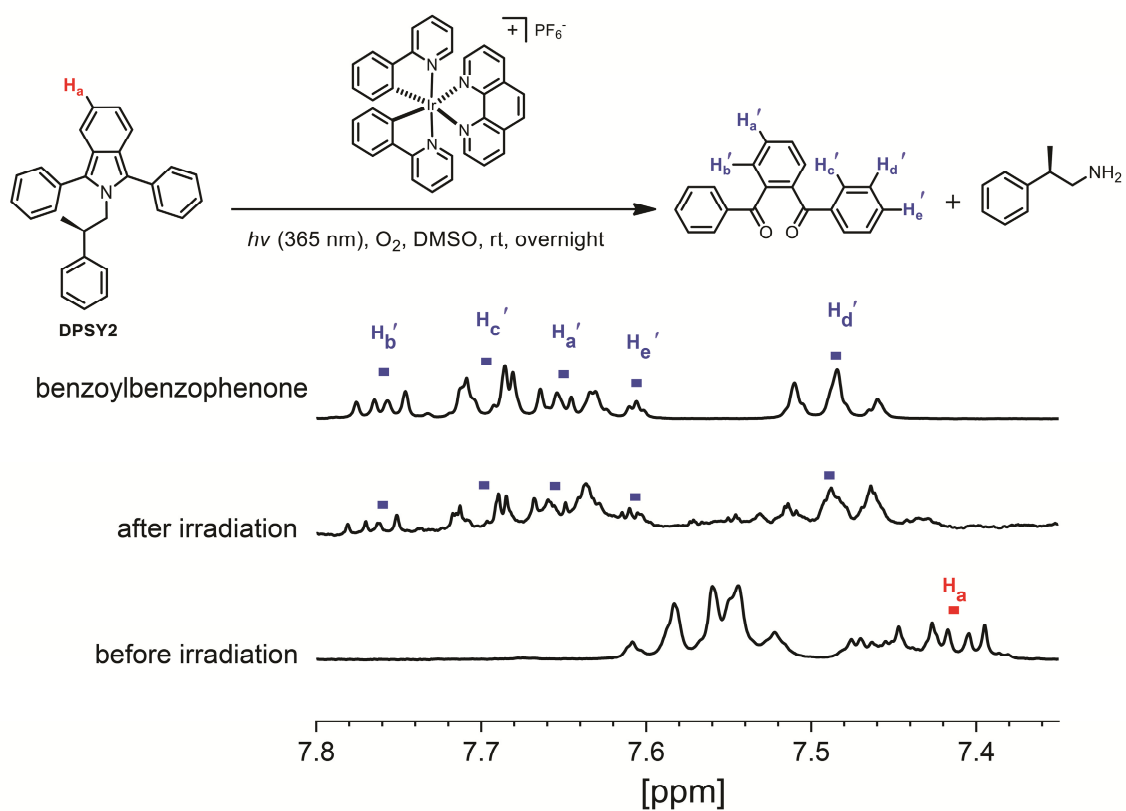


**Fig. S4** <sup>1</sup>H NMR spectra (300 MHz) of DMSO-*d*<sub>6</sub> containing 3.0 mM DPSY2 and 100 μM Irppy before (bottom) and after (middle) photoirradiation at a wavelength of 365 nm for 20 h. The <sup>1</sup>H NMR spectrum of 6.0 mM 2-benzoylbenzophenone (top) is included for comparison. See the reaction scheme at the top for the peak assignments.

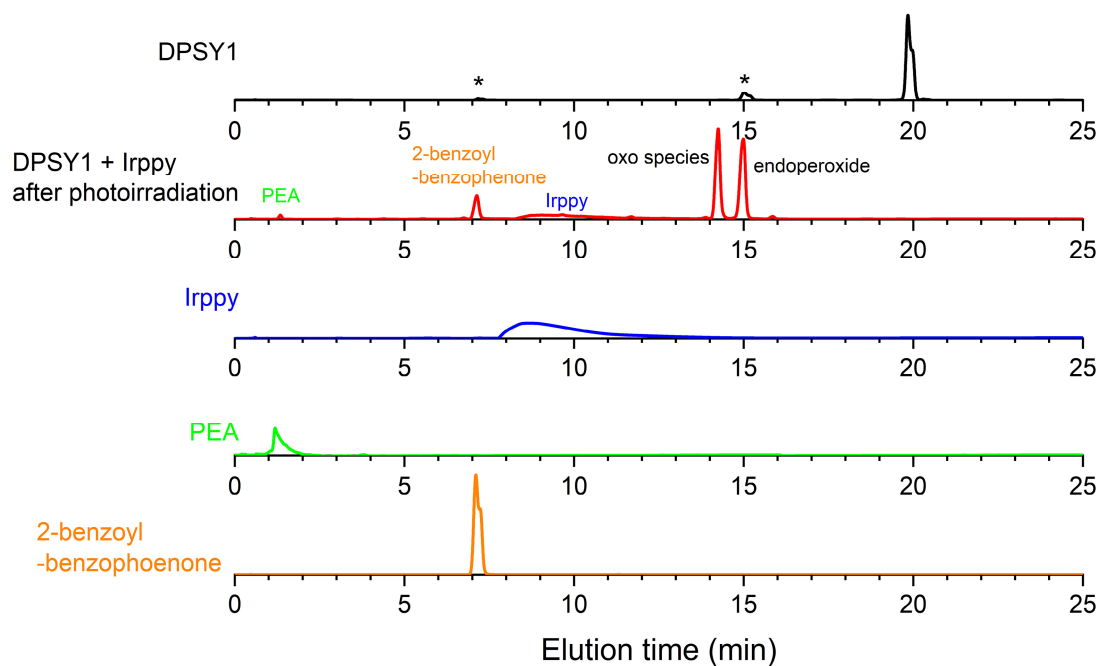


**Fig. S5** Liquid chromatograms (UV detection at 254 nm) of 1.0 mM DPSY1 (black), the photolyzed (25 min, 365 nm) solution of an O<sub>2</sub>-saturated CH<sub>3</sub>CN containing 1.0 mM DPSY1 and 100 μM Irppy (red), 200 μM Irppy (blue), 1.0 mM PEA (green), and 1.0 mM 2-benzoylbenzophenone (orange). Peaks marked with asterisks are the photoproducts.

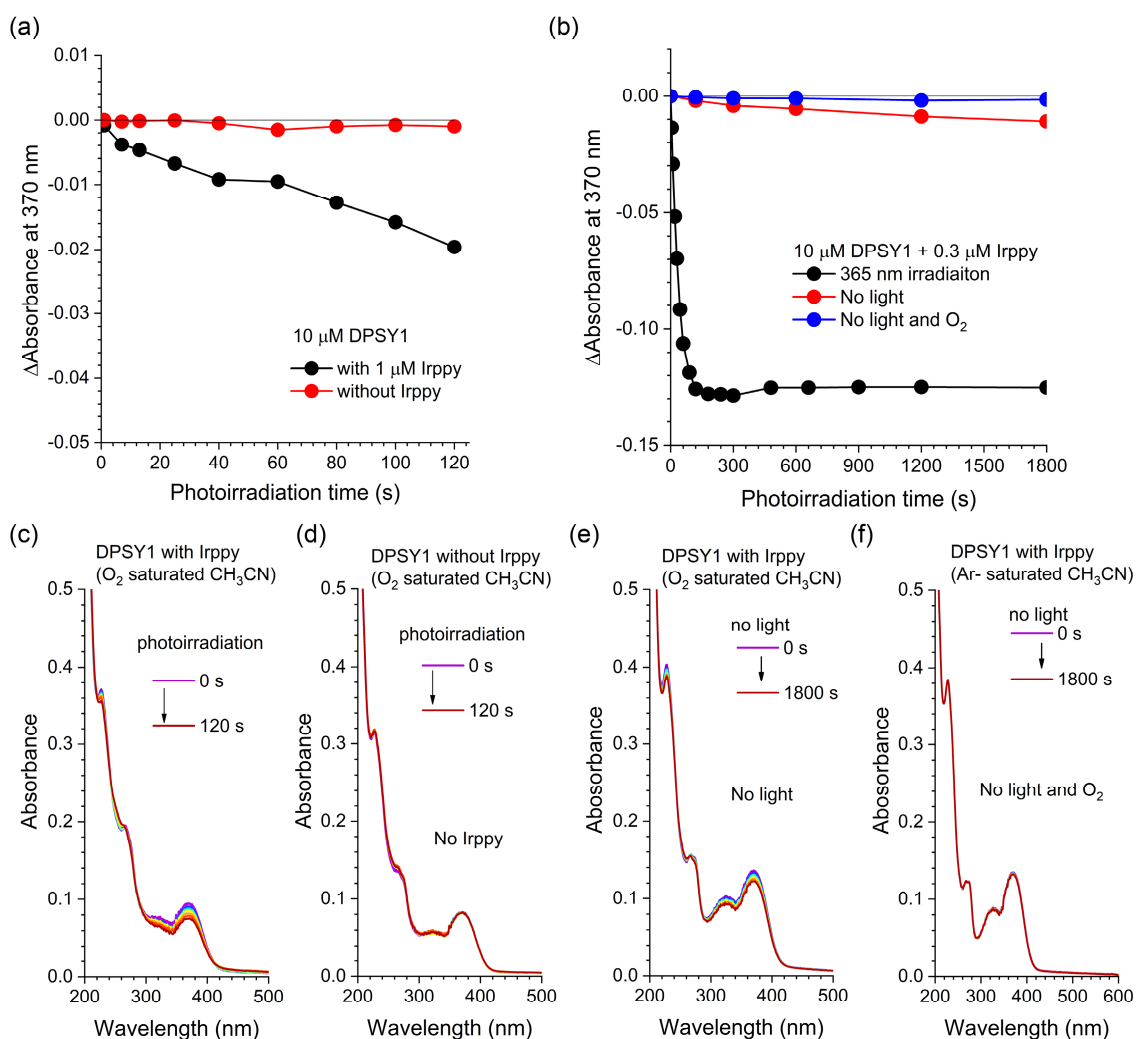


**Fig. S6** Control experiments of the photocaging of PEA from 10 μM DPSY1 (CH<sub>3</sub>CN). (a) Absorbance difference at a wavelength of 370 nm monitored during continuous photoirradiation in the presence (black) and absence (red) of 1 μM Irppy. See (c,d) for the spectral evolutions. (b) Absorbance difference at a wavelength of 370 nm monitored during continuous photoirradiation (black) and under dark after aeration (red) and after deaeration (blue). See (c,e,f) for the spectral evolutions. (c–f) Changes in the UV–vis absorption spectra of CH<sub>3</sub>CN solutions containing 10 μM DPSY1 under various conditions.

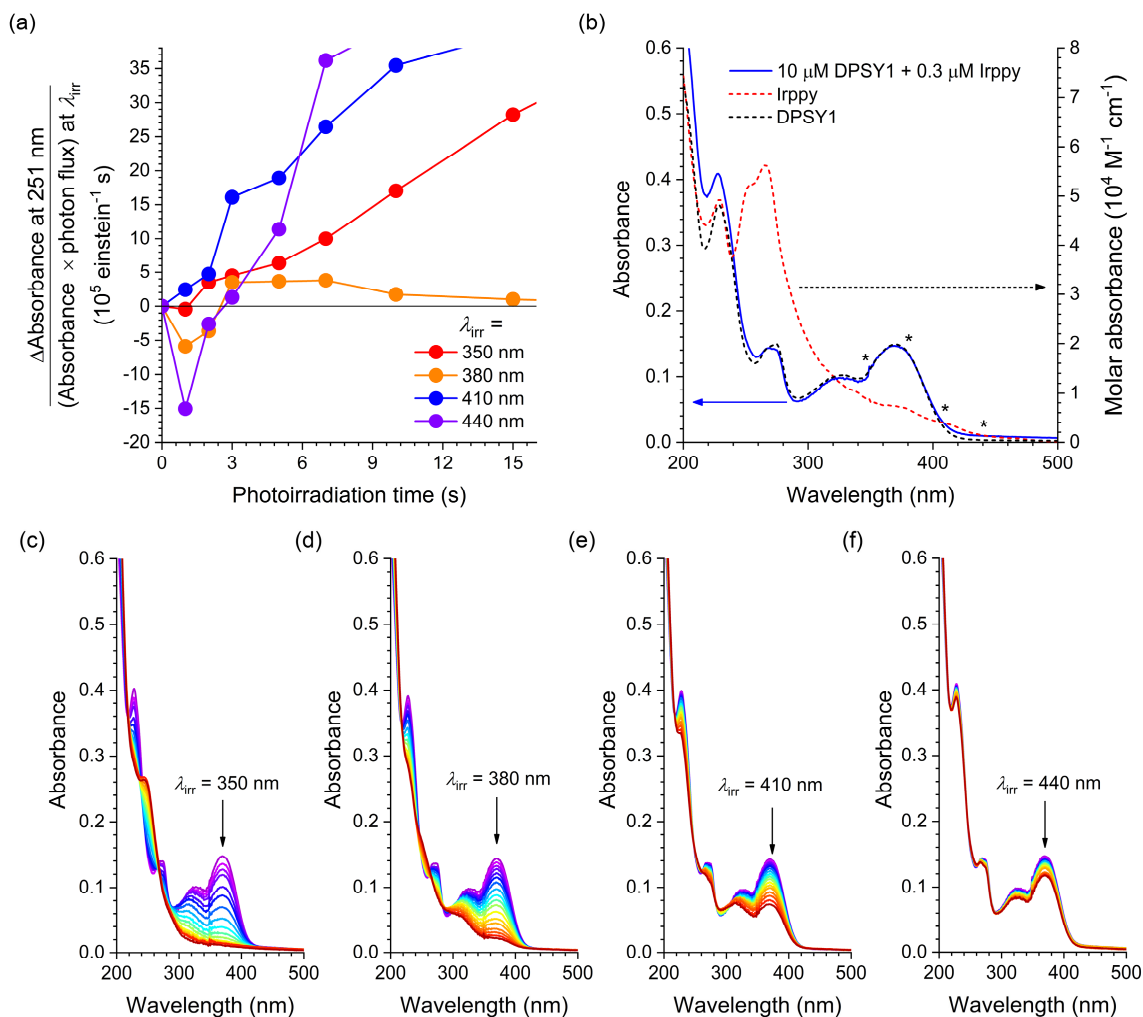


**Fig. S7** Variable-wavelength photocaging of  $O_2$ -saturated  $CH_3CN$  containing  $10 \mu M$  DPSY1 and  $0.3 \mu M$  Irppy. (a) Absorbance difference at a wavelength of 251 nm monitored during continuous photoirradiation with monochromatic lights of 350, 380, 410, and 440 nm. See (c–f) for the spectral evolutions. Note that the absorbance difference was corrected with photon absorption by dividing the value with the absorbance value of the mixture and the photon flux at each photoirradiation wavelength. Photon flux was determined using an optical power meter to be  $12 \times 10^{-8} \text{ einstein s}^{-1}$  at 350 nm,  $3.8 \times 10^{-8} \text{ einstein s}^{-1}$  at 380 nm,  $4.3 \times 10^{-8} \text{ einstein s}^{-1}$  at 410 nm, and  $4.9 \times 10^{-8} \text{ einstein s}^{-1}$  at 440 nm. (b) Comparison of the UV–vis absorption spectra of Irppy (red dotted line), DPSY1 (black dotted line), and the mixture of  $10 \mu M$  DPSY1 and  $0.3 \mu M$  Irppy (blue solid line). The asterisks indicate the positions of the monochromatic lights. (c–f) Changes in the UV–vis absorption

spectra of the O<sub>2</sub>-saturated CH<sub>3</sub>CN containing 10 μM DPSY1 and 0.3 μM Irppy recorded during photoirradiation at wavelengths of 350 nm (c), 380 nm (d), 410 nm (e), and 440 nm (f).

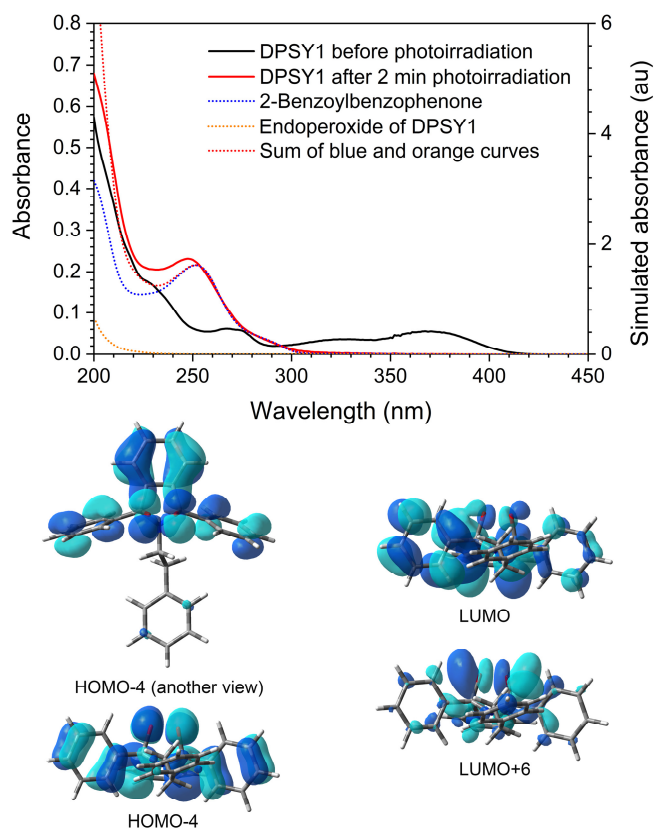


**Fig. S8** Comparisons of the experimental absorption spectra of 10 μM DPSY1 before (black curve) and after (red solid curve) 2-min photoirradiation and 10 μM 2-benzoylbenzophenone (blue dotted curve) with the simulated (TD-CAM-B3LYP/6-311+G(d,p)) electronic transition spectrum for the endoperoxide of DPSY1 (orange dotted curve). The mathematical sum of the spectra of 10 μM 2-benzoylbenzophenone and the endoperoxide is included (red dotted curve). The close match between the sum spectrum (red dotted curve) and the experimental spectrum for the 2-min-photolyzed DPSY1 (red solid curve) suggests the conversion of DPSY1 into 2-benzoylbenzophenone or the endoperoxide. The bottom images displays the isosurface plots of the molecular orbitals involved in the electronic transition for the lowest singlet state of the endoperoxide ( $S_1$ , HOMO-4  $\rightarrow$  LUMO (0.24) + HOMO-4  $\rightarrow$  LUMO+6 (0.30)). Note that the LUMO and LUMO+6 involve the  $\sigma^*$  orbitals between the two oxygen atoms in the endoperoxide.

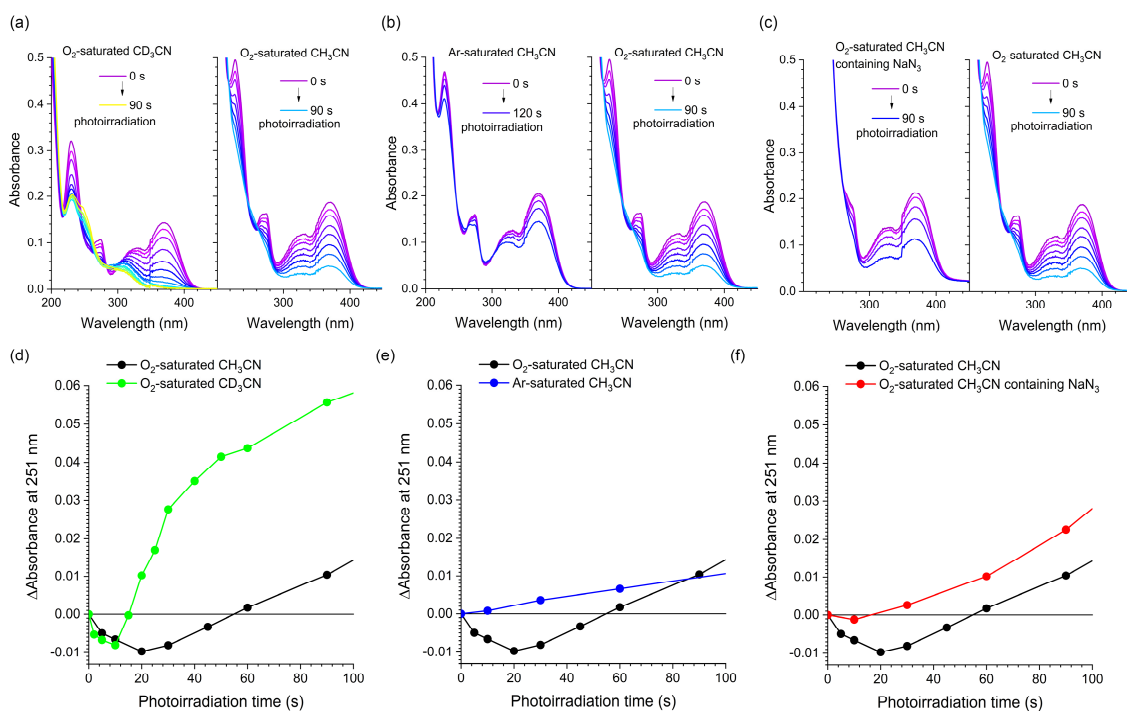


**Fig. S9** (a) Comparisons of the changes in the UV-vis absorption spectra of  $O_2$ -saturated  $CD_3CN$  (left) with those of  $O_2$ -saturated  $CH_3CN$  (right) monitored under photoirradiation at 365 nm. (b) Comparisons of the changes in the UV-vis absorption spectra of Ar-saturated  $CH_3CN$  (left) with those of  $O_2$ -saturated  $CH_3CN$  (right) monitored under photoirradiation at 365 nm. (c) Comparisons of the changes in the UV-vis absorption spectra of  $O_2$ -saturated  $CH_3CN$  containing 100 mM  $NaN_3$  (left) with those of  $O_2$ -saturated  $CH_3CN$  (right) monitored under photoirradiation at 365 nm. (d-f) The corresponding temporal changes of the absorbance difference at 251 nm: (d) Absorbance difference changes at 251 nm of the spectra of (a), (e) absorbance difference changes at 251 nm of the spectra of (b), and (f) absorbance difference changes at 251 nm of the spectra of (c).

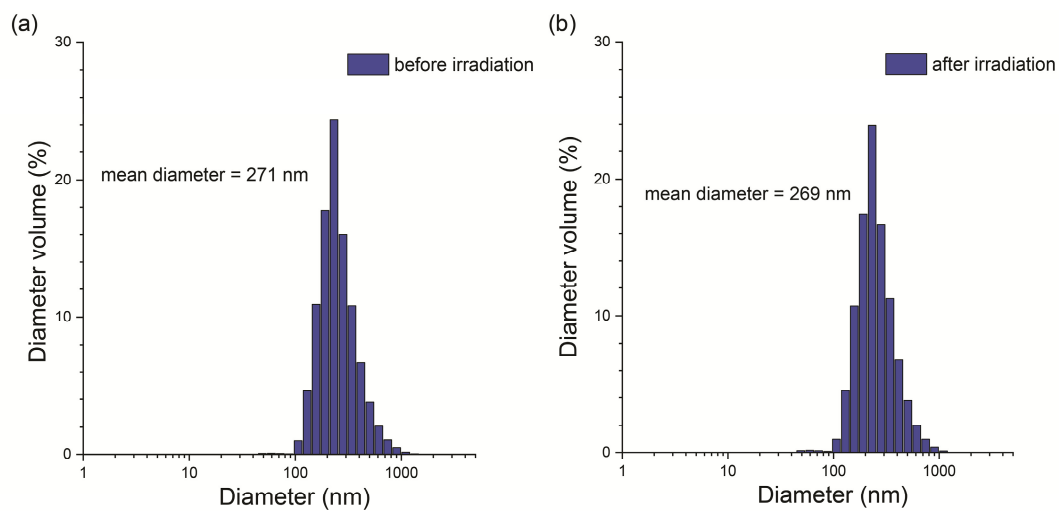


**Fig. S10** Distributions of the diameter of the DMPC liposomes before (a) and after (b) photoirradiation at a wavelength of 365 nm for 25 min. The liposomes were doped with 0.01 wt % DPSY1 and 0.05 wt % Irppy. The peak diameters were 271 and 269 nm for the liposomes before and after, respectively, of photoirradiation.

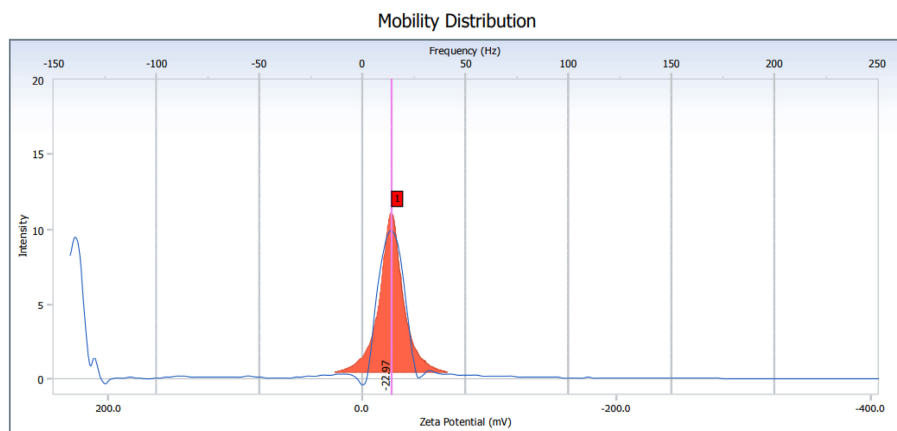


**Fig. S11** Surface charge of the DMPC liposomes doped with 0.01 wt % DPSY1 and 0.05 wt % Irppy. The surface charge was  $-22.97$  mV.

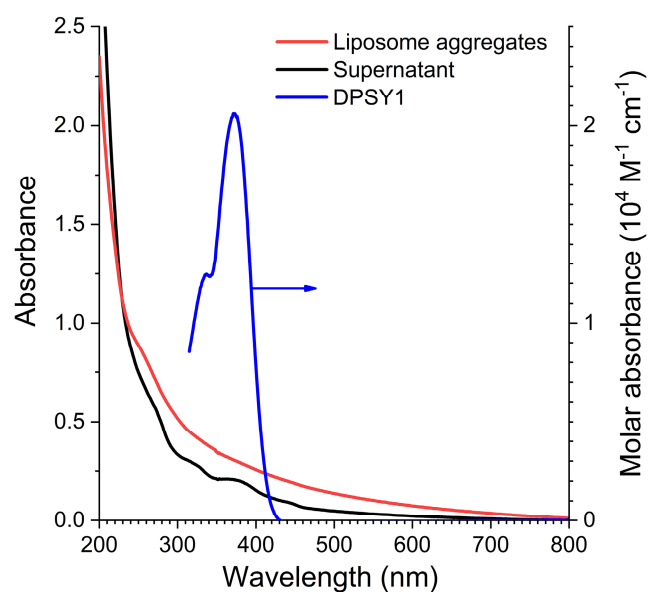


**Fig. S12** Determination of an efficiency for the encapsulation of DPSY1 within the DMPC liposomes. As-prepared DMPC liposome suspension was centrifuged for 30 min at 2000 rpm and 20°C. Supernatant and liposome aggregates were separated, and their UV-vis absorption spectra were taken. The efficiency of encapsulation is calculated through a relationship, efficiency of encapsulation (%) =  $100 \times (\text{absorbance}(372 \text{ nm}) \text{ of liposome aggregates}) / (\text{absorbance}(372 \text{ nm}) \text{ of liposome aggregates} + \text{absorbance}(372 \text{ nm}) \text{ of supernatant})$ . The red and black curves correspond to the UV-vis absorption spectra of the liposome aggregates and supernatant, respectively. The UV-vis absorption spectrum of DPSY1 is included (blue curve).

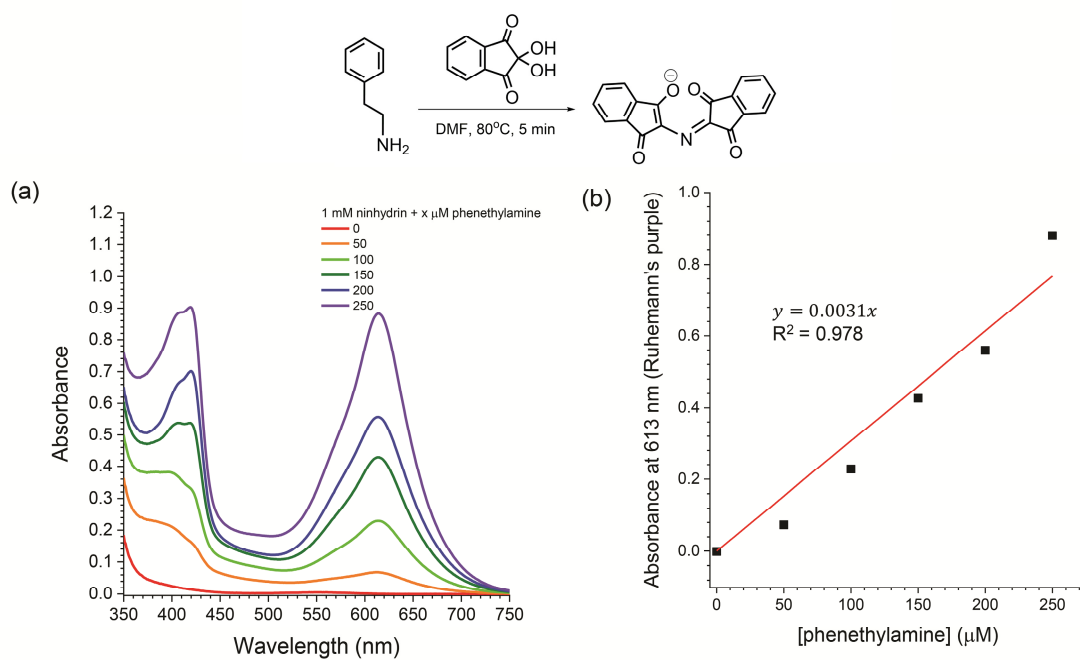


**Fig. S13** Calibration curve of the ninhydrin test for  $\beta$ -phenylethylamine. (a) UV-vis absorption spectra of 1 mM ninhydrin reacted with varied concentrations of  $\beta$ -phenylethylamine (0, 50, 100, 150, 200, and 250  $\mu\text{M}$ ) in DMF. (b) A linear fit of the absorbance of Ruhemann's purple at 613 nm as a function of the concentration of  $\beta$ -phenylethylamine ([phenethylamine],  $\mu\text{M}$ ). The reaction scheme is shown on top.

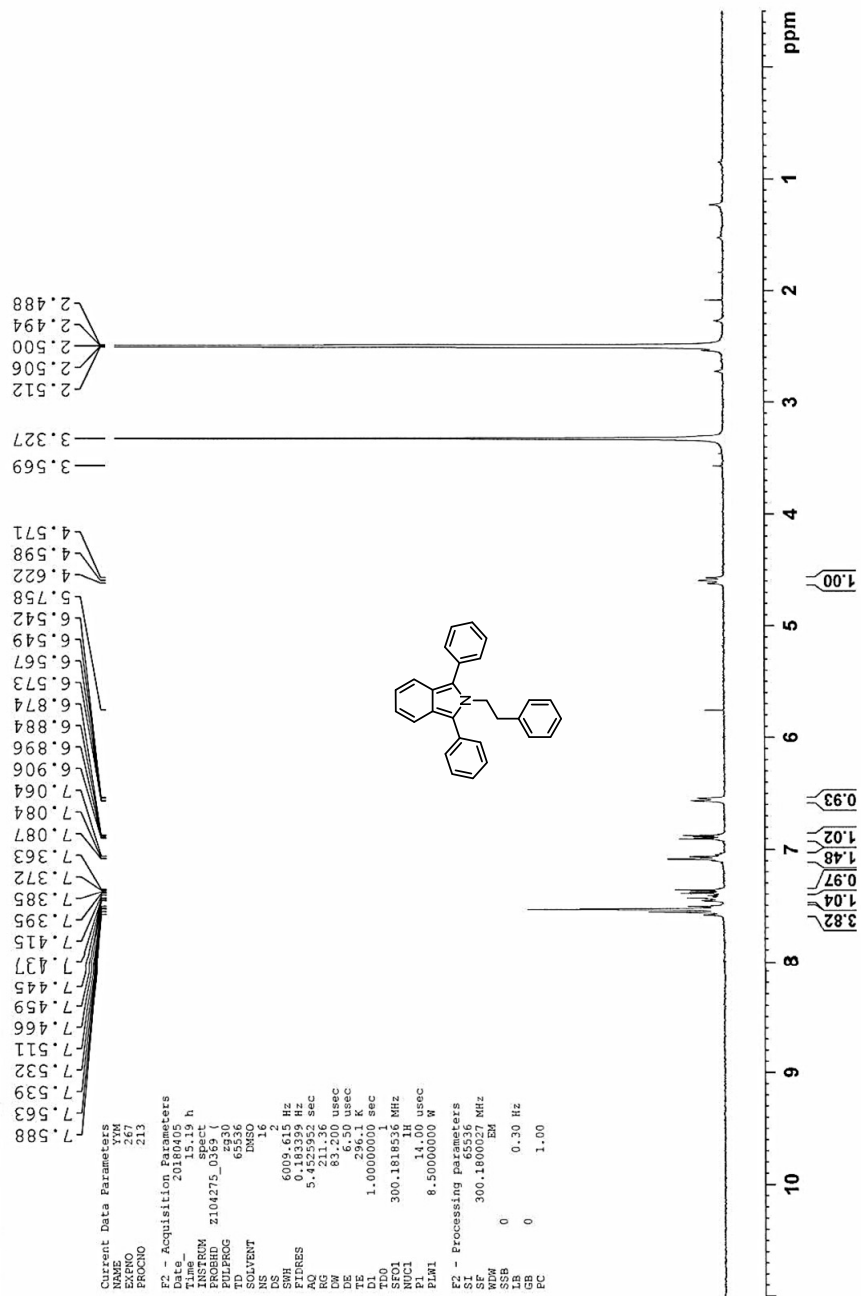


Fig. S14 <sup>1</sup>H NMR (300 MHz, CD<sub>2</sub>Cl<sub>2</sub>) spectrum of DPSY1.



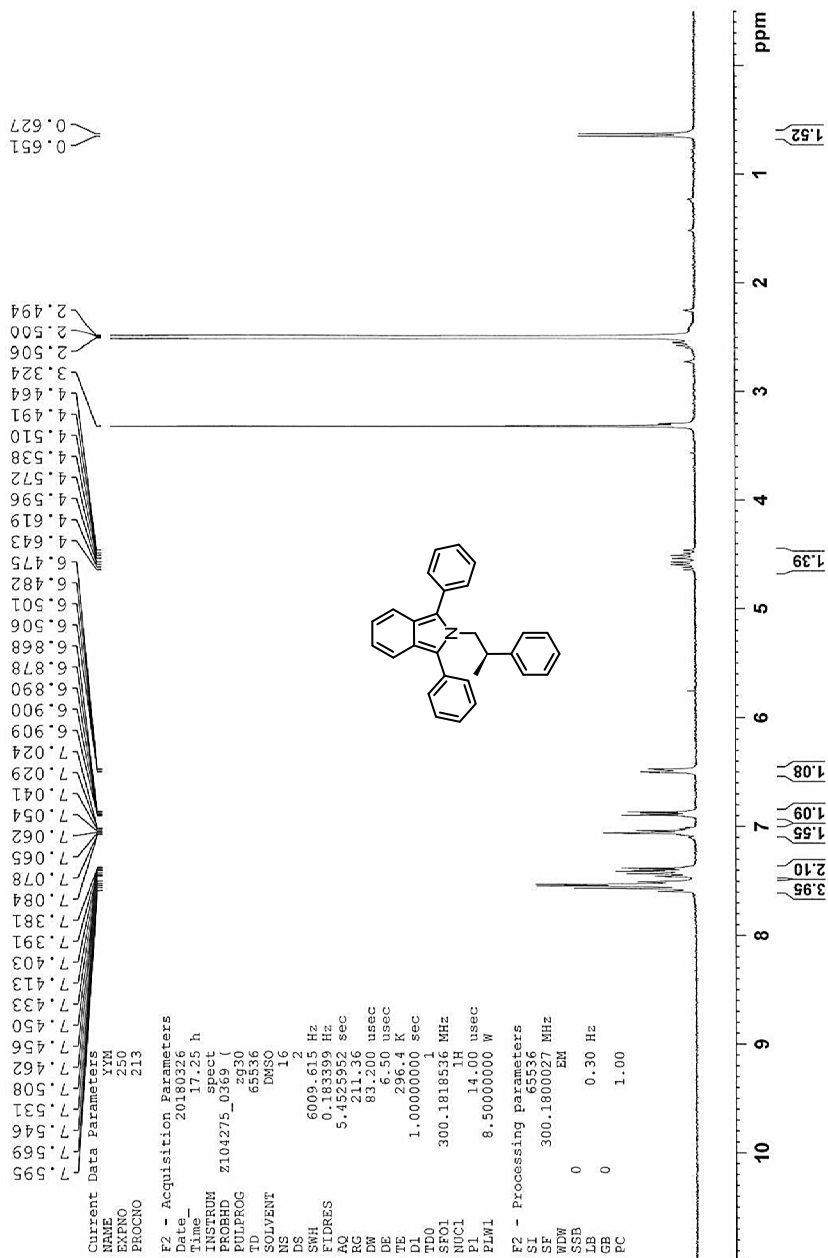


Fig. S16 <sup>1</sup>H NMR (300 MHz, DMSO-*d*<sub>6</sub>) spectrum of DPSY2.

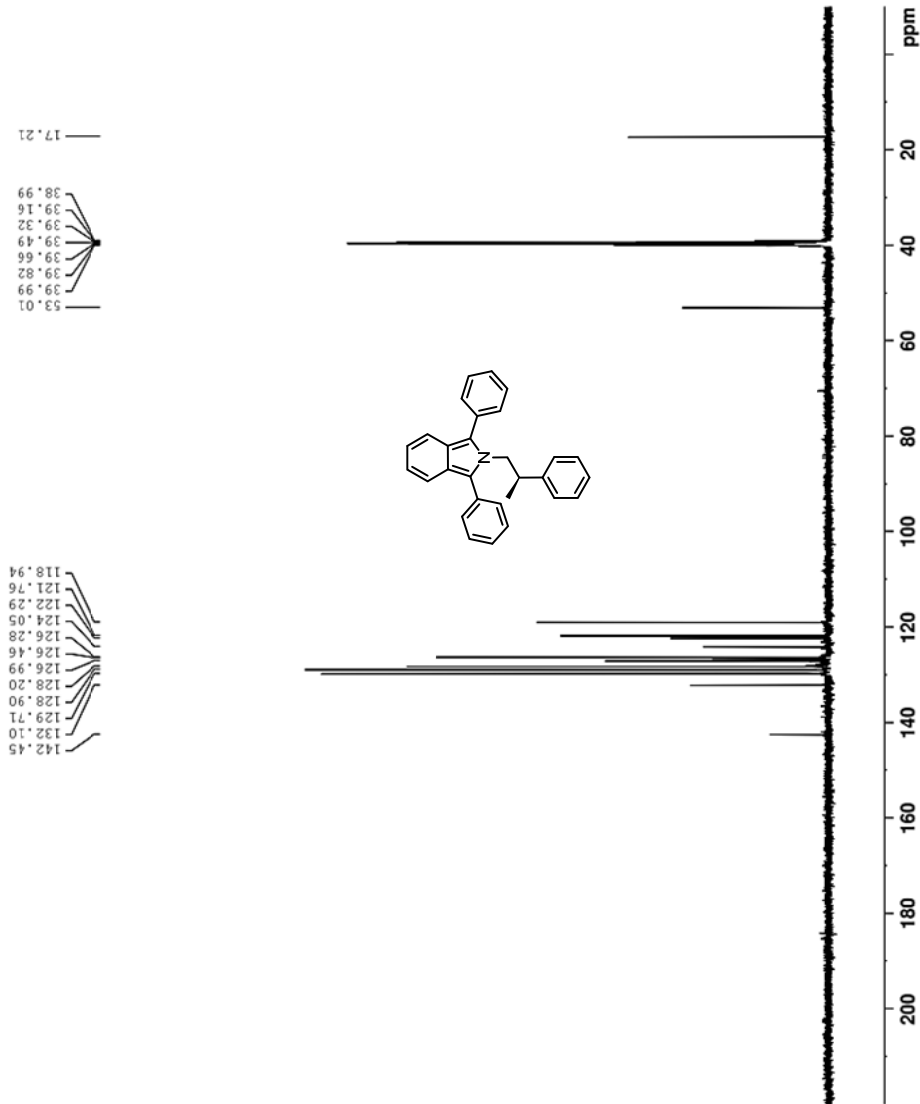


Fig. S17  $^{13}\text{C}\{^1\text{H}\}$  NMR (126 MHz,  $\text{DMSO-}d_6$ ) spectrum of DPSY2.